Dermarob: A Safe Robot for Reconstructive Surgery

Etienne Dombre, *Member, IEEE*, Gilles Duchemin, Philippe Poignet, and François Pierrot, *Senior Member, IEEE*

***Abstract*—This paper presents a novel and safe robotic system for skin harvesting, the first one in reconstructive surgery. It is intended to significantly improve the performance of surgeons who do not regularly perform this operation; the tool, called dermatome, is mounted at the tip of a dedicated robot that precisely controls the pressure on the skin and the harvesting velocity. In this paper, the harvesting task is analyzed and the safety constraints are summarized. Then, the mechanical structure and the functions of the control system are described. Finally, *in vivo* experimental results on pigs are reported and discussed.**

***Index Terms*—Medical robot, reconstructive surgery, skin harvesting.**

I. Introduction

SKIN harvesting from the human body for grafting purposes requires highly accurate gestures and is physically very demanding for the surgeon, due to the efforts he has to exert. This technique aims at harvesting a constant thickness strip of skin (a few tenths of millimeter) with a "shaver-like" device, called *dermatome* (Fig. 1). It requires a long period of training and has to be regularly practiced (for instance, for orthopedic physicians, this gesture may not be completely mastered, as it is not a daily operation). According to the burn degree, skin strips may be harvested from different locations on the patient, mainly thighs, buttocks, head (thus, scars may be hidden by hair). Because of their shape, some of these locations are more difficult to harvest. These features have been analyzed and justify the robotization of skin harvesting in reconstructive surgery. The goal of the "Système de Coupe Automatisé pour Le Prélèvement de Peau" (SCALPP) project is to embed part of a specialized surgeon skill in a robotic system (a.k.a., the commercial name of Dermarob). Thus, this skill will be brought to other surgeons who do not regularly practice skin harvesting. This project is run together with Lapeyronie Hospital in Montpellier, France, and SINTERS, a French engineering company.

The closest application to skin harvesting that was ever robotized was probably sheep shearing in the 1970s, thanks to the well-known Oracle robot, later improved by the Shear Magic robot [1]. However, the clippers had to be kept at a safe distance from the skin and the difficulty was more to predict the paths covering all the surface to be shorn, and to manipulate the sheep into the shearing positions. In the medical field, the closest devices are our Hippocrate system [2] and the ultrasound robot from UBC [3], both dedicated to performing ultrasound artery examinations. With the former, the probe applies a constant force on the skin along a discretized point-to-point path. In the SCALPP project, the force applied is much higher, deforming the skin along a continuous path.

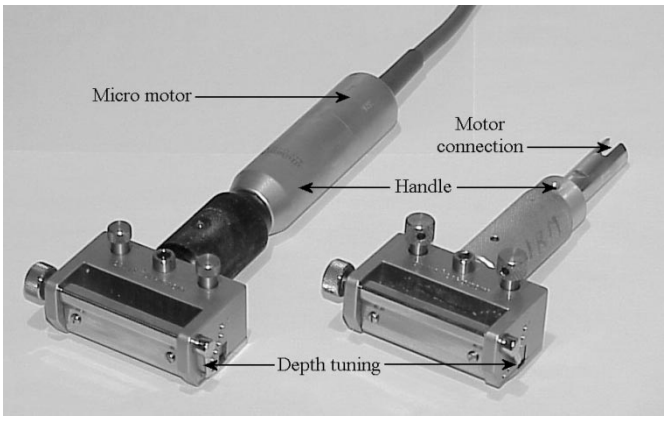

Fig. 1. Two models of dermatome: (left) embedded motor; (right) remote motor; the blade is underneath.

This paper describes the approach which has led to the design of the Dermarob system: a task analysis has been done with surgeons performing on pigs, and feasibility experiments have been run with a PA-10 robot, showing that the task could be robotized with an appropriate position-force control scheme (Section II). However, due to safety requirements, we have chosen to design a novel robotic system instead of refitting an industrial one, as justified in Section III. The safety constraints have been analyzed and translated in terms of mechanical, hardware, and software specifications. These specifications combined with the desired geometric and kinematic performances have resulted in the mechanical design described in Section IV and the control architecture described in Section V. The project is currently in the assessment phase on pigs. Experimental results are presented and discussed, respectively, in Sections VI and VII.

II. Task Analysis

As with most human motions, it is extremely difficult to accurately model the surgeon's gesture when harvesting skin, in terms of kinematics and force [4]. The motion is a three-dimensional (3-D) one, combined with quite large forces exerted on a nonmodeled and soft surface. The aforesaid softness depends on the bones and tissues underneath. The force and velocity produced by the surgeon depend on various parameters: patient's skin, fatigue, training, etc.

Manuscript received June 17, 2002; revised December 23, 2002. This paper was recommended for publication by Associate Editor J. Troccaz and Editor R. Taylor upon evaluation of the reviewers' comments. This work was supported in part by the French Ministère de l'Education Nationale et de la Recherche and the Région Languedoc-Roussillon. This paper was presented in part at ICAR, Budapest, Hungary, 2001, and in part at ISER, San Angelo, Italy, 2002.

E. Dombre, P. Poignet, and F. Pierrot are with LIRMM, 34392 Montpellier Cedex, France (e-mail: dombre@lirmm.fr; poignet@lirmm.fr; pierrot@lirmm.fr).

G. Duchemin was with Sinters, Parc Technologique Basso Cambo, 31106 Toulouse Cedex 1, France. He is now with LIRMM, 34392 Montpellier Cedex, France (e-mail: duchemin@lirmm.fr).

Digital Object Identifier 10.1109/TRA.2003.817067

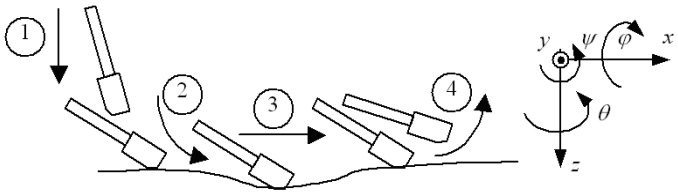

Fig. 2. Four steps of the skin harvesting process with a dermatome.

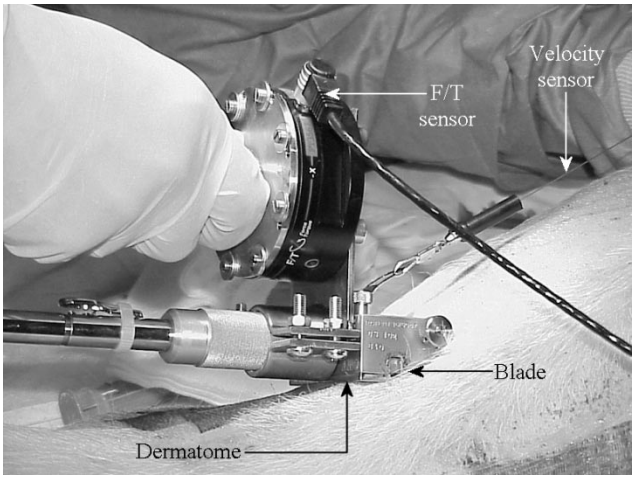

Fig. 3. Surgeon performing skin harvesting on a pig.

A feasibility study [4] has shown that the surgeon motion could be divided into four steps (Fig. 2). During the initialization step (step 1), after the contact is reached, the surgeon orients the dermatome about the y axis and presses it along the z axis (normal to the skin) in such a way that the blade penetrates the skin; when the first cut is obtained, he reorients the dermatome about the y axis so that the blade plane comes into full contact with the skin (step 2); in these two steps, there has to be as little motion along the x axis as possible; then, the harvesting process begins, consisting in a motion along the x axis while the blade plane is kept against the skin with a roughly constant contact force (step 3); finally, the surgeon frees the dermatome by doing a quick rotation about the y axis (step 4).

Experiments have exhibited that during step 3, the contact force exerted by the surgeon along z ranges from 40 N up to 100 N; the torque about x is roughly zero, meaning that the surgeon keeps the dermatome blade in close contact with the skin. The harvesting velocity is lower than 5 cm.s^{-1}. Fig. 3 shows the experimental set-up: a six-component force/torque (F/T) sensor (Gamma F/T transducer from ATI) is inserted between the surgeon's hand and the dermatome; the velocity is measured along x using a wire rope transducer (ASM Sensor) attached to the dermatome. This set-up is rather cumbersome, but proved to be satisfying to evaluate rough ranges of variation of force and velocity. Two strategies have been exhibited from the analysis gathered from the experimental data, depending on whether the velocity is kept constant over the step 3. In one strategy, the velocity is modified according to the force along x, but then, the fact that the power dissipated along this direction (computed as the product $F_x\dot{x}$) is almost constant can be verified. Another strategy for the surgeon is to keep a constant velocity.

Besides, the cutting depth of the dermatome is mechanically limited (Fig. 1). Therefore, and up to a certain threshold value, the thickness of the skin graft depends on the normal force exerted. The surgeon adapts his force to a value beyond this threshold to make sure that the skin graft will have a regular shape and no hole. The threshold value depends on the patient and on the nature of tissues underneath the harvesting location.

Finally, the feasibility study [4] has also shown that it is mandatory to control the contact force component F_z and moment components M_x, M_y, which require an actuated arm. Besides, the complex motion of the dermatome against the skin requires six degrees of freedom (DOF).

III. Safety Issues

The key objective of medical robotics is to design, manufacture, and control intelligent devices aimed at improving health care and quality of life [5]. But one of the major characteristics of medical robots is also to strongly interact with human environment (i.e., with possibly trained and/or (especially) not trained people who can have unpredictable behavior).

Robots in the industry are usually isolated from the workers who receive an appropriate training to interact with them. This is completely different in the operating room (OR). In [6], the authors state the constraints of a surgical environment: 1) the work has to be done on a human being with soft tissues; 2) the environment is usually unstructured; 3) each task and its execution is specific to the patient; 4) the robot has to be transportable in and out of the OR; 5) its dimensions have to be reduced; and finally, 6) each component has to be sterilized.

The first robots used in surgery were industrial robots modified to increase their safety [7], [8]. Today, from a safety point of view, mechanical arms involved in medical robotic applications are of three types depending on their level of autonomy [9]: 1) passive arms, that are nonactuated and have no autonomy; 2) semiactive arms for which the contact force is produced by the surgeon, not by the robot; thus, either the power is cut off during critical phases of the tasks (Neuromate from ISS), or the actuators are used to constrain certain directions of displacement. This is done by reflecting a variable force to the surgeon, for instance in PADyC [9] or Acrobot [10]; and 3) active arms where most of the joints are actuated, thus performing part of planned tasks on their own (Robodoc from ISS, Caspar from URS Ortho, etc.) or in a teleoperated mode (Zeus from Computer Motion, da Vinci from Intuitive Surgical).

As mentioned in Section II, skin harvesting requires force control, thus an active robot. Such a robot should ensure a high level of safety in order to be used in an OR. As suggested by Davies [5], a medical device should be designed considering the following principles.

1) Redundancy in control and sensing. However, redundancy raises the number of components, thus increasing the complexity of the system, which finally decreases its reliability.
2) Intrinsic safety obtained with classical components such as actuators with limited power and/or speed; high-reduction gears such as harmonic drives (for their low backlash and flexibility and for their high efficiency); a "Dead Man

Switch" (DMS) foot pedal, used by the surgeon to authorize motion of the robot; watchdog board checking the activation of the control system.

In Dermarob, both approaches have been combined [2], [11]. Specific mechanical, hardware, and software features have been added to provide an intrinsic reliability and safety to the whole system, as emphasized in Sections IV and V.

IV. Mechanical Design

Kinematic and geometric dimensions of Dermarob have been specified with following various constraints.

1) For asepsis considerations, no nonmedical equipment must be closer than 400 mm to the operating table.
2) The length of a zone to harvest may vary from a few millimeters to 400 mm (which corresponds to the length of a thigh); the orientation change of the dermatome may be up to 90° about the y axis (when harvesting a skull), and a few degrees about the z axis (Fig. 2).
3) The robot might be set up on either side of the operating table. Thus, symmetrical joint limits would be preferred.
4) Good accessibility to the dermatome handle is needed.
5) The robot should be able to move along a path without crossing singularities and reaching joint limits.

Under these constraints, a dedicated architecture has been designed [12]. Two types of shoulders were first considered: anthropomorphic and SCARA. Anthropomorphic architectures present two main drawbacks for the application at hand: their workspace is spherical; and under gravity effect, the robot could collapse and hurt the patient, especially if a power cutoff occured. The advantage of a SCARA shoulder is that its cylindrical workspace is less wasteful, and the gravity may be compensated by a simple counterweight if the prismatic joint is the first joint of the shoulder (no specific brakes are required). Finally, a CAD study has shown that the accessibility to the points of typical harvesting paths was better with a SCARA than with an anthropomorphic shoulder of equivalent link lengths. Therefore, a SCARA architecture has been preferred. One could then wonder which axis would be made prismatic, since the first, third (or fourth), and sixth are possible candidates. This robot was designed with the first joint prismatic for the following reasons: as aforementioned, gravity is easy to compensate; the accessibility to the dermatome handle for the surgeon is better; and the volume swept by the arm during motion is more compact and regular since it does not depend on extension of a last translation. It can be argued that the prismatic joint carries the entire weight of the robot, which makes good force control more difficult to achieve along the vertical direction. However, this is not critical, since the forces exerted by the dermatome are not restricted to this direction.

We have also evaluated the advantages of placing the robot either on a track fixed to the ceiling, or on a support on the ground. A surgery room is usually cluttered with many pieces of equipment and some of them are already hung from the ceiling, thus discarding the ceiling-mounted solution.

For the wrist, different nonspherical architectures have been investigated. Their advantage is to eliminate the classical singularity of the spherical ones when fully extended [12], as Trevelyan already did for the Oracle robot [1]. The wrist presented in Fig. 4 validates this constraint since the only singularity appears on the fifth joint when θ_5 reaches $\pm$ 90°, while providing sufficient joint range.

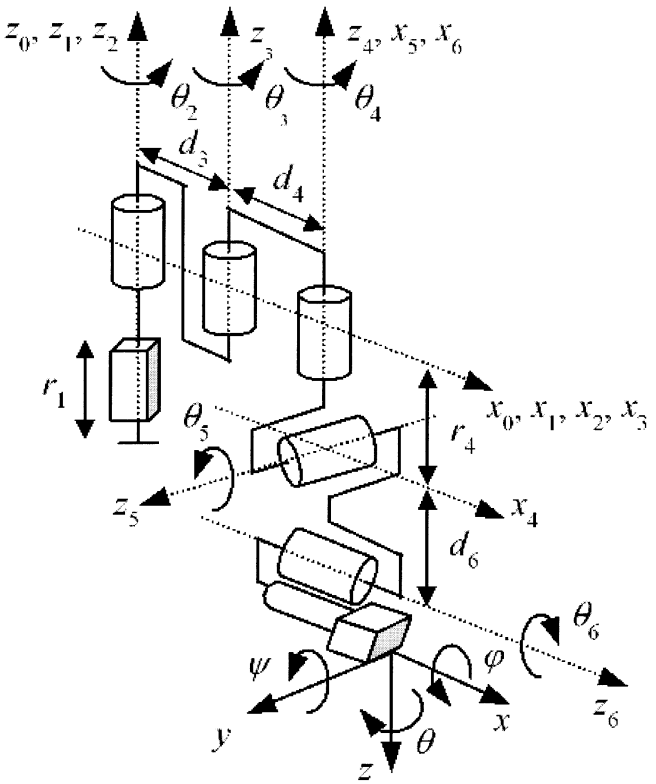

Fig. 4. Geometric architecture of the shoulder and the wrist.

TABLE I
Modified Denavit–Hartenberg Parameters [14] for Dermarob

j	α_j	d_j	θ_j	r_j
1	0	0	0	r_1
2	0	0	θ_2	0
3	0	400	θ_3	0
4	0	400	θ_4	345
5	$\pi/2$	0	$\theta_5 + \pi/2$	0
6	$\pi/2$	110	θ_6	0

Length in mm.

As a consequence, Dermarob features a single singularity in the workspace (when $\theta_3 = 0$, i.e., when the arm is fully extended). A closed-form solution for the inverse geometric model (IGM) does exist, since the robot has a prismatic joint and a revolute joint with parallel axes [13]. Theoretically, four solutions result from the IGM computation, but two of them are out of the joint limits and only two configurations are available ("left elbow" or "right elbow"). The equations of the direct and inverse geometric models can be found in [12].

The dimensions of the arm, expressed with a modified notation of Denavit–Hartenberg as defined in [14], are given in Table I. The arm is mounted on a mobile cabinet containing the controller as shown in Fig. 5. Specifications of Dermarob are given in Table II.

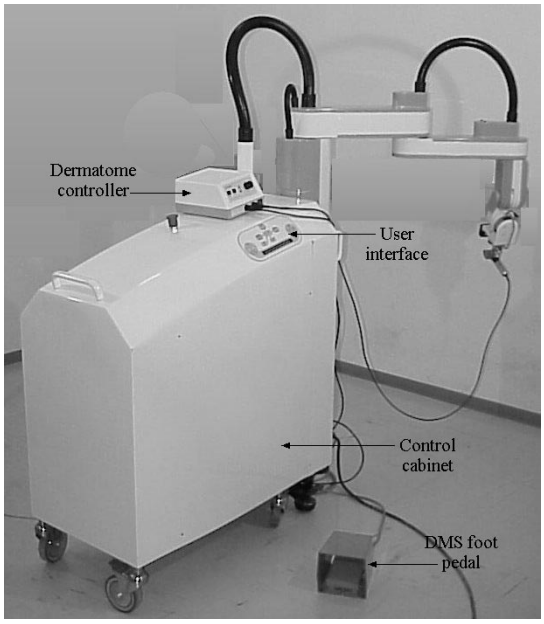

Fig. 5. Dermarob arm and the control cabinet.

TABLE II
SPECIFICATIONS OF DERMAROB

Controlled axes		6 axes: PRR-RRR	
Motion range (Maximum velocity)	r_1	400 mm	(100 mm/sec)
	θ_2	240°	(10 °/sec)
	θ_3	300°	(15 °/sec)
	θ_4	440°	(60 °/sec)
	θ_5	140°	(60 °/sec)
	θ_6	150°	(80 °/sec)
Maximum velocity at the tool tip		100 mm/sec	
Maximum load capacity at wrist		130 N	
Maximum load moment at wrist		25 Nm	
Repeatability along z		0.1 mm	
Resolution		0.02 mm	
Weight	Arm	55 Kg	
	Control cabinet	200 Kg	

Safety constraints have led us to choose suited technological components as follows.

1) Each motor has been chosen to minimize the power transmitted at the joint level.
2) The reduction ratios of the harmonic drives range from 120 up to 160.
3) Stepper actuators have been selected: the main reason is that with conventional dc or ac motors, the rotation speed of the shaft depends on the voltage output level of the servo amplifier. If a fault occurs, the motor still goes on rotating. On the contrary, stepper actuators need pulse to rotate. If the output of a translator is stuck to a constant value, the motor shaft would receive a holding torque, preventing it from rotating. These stepper motors have a high resolution thanks to a microstep control mode (resolution of 64 microsteps for each step). The motors selected have 200 steps per revolution, providing a 0.028°/microstep resolution. Therefore, with a reduction ratio of 160, the theoretical resolution is better than 0.003 mm. Practically, the use of stepper motors does not affect the global resolution of the robot (0.02 mm as indicated in Table II).
4) Joints 2–5 are equipped with two absolute sensors (resolvers) per joint, one mounted on the motor output shaft for fine position sensing, and the other one mounted on the output reduction gear for coarse sensing. This combination of resolvers suppresses time consuming and potentially hazardous initialization procedures.
5) The cables are embedded in the wrist.
6) The shoulder is backdrivable, thus quickly and easily removable from the operating field.

V. CONTROL SYSTEM

The control system is stacked in a compact cabinet mounted on wheels which can be easily moved in and out of the OR. It contains four racks: one with a 550-MHz Pentium industrial PC running under the Real Time and Multitasking Operating System (RTMOS) QNX for the high-level control; another with the resolver and translator boards for the control of the stepper actuators; a power supply rack; and the last one with the logical unit formatting the input/output (I/O) signals between the user interface (UI), the switches, the light signals, and PC boards.

A. UI and Operating Modes

The UI has been developed in close cooperation with surgeons in order to provide user-friendly tools for the robotic system. It consists of three main control structures: a console desk that enables bilateral communications between the user and the robot; it is made up of three sets of control buttons: one to cancel and validate actions (`esc.` and `enter`), another to decrement and increment force applied on skin ($-$ and $+$) and a last one to control the arm (`start`, `free` and `reconfig.`); several lights (`powered`, `active`, and `fault`) and an LCD display that indicates the current mode and the faults detected; and a DMS that authorizes arm motion.

A careful analysis of the skin harvesting task has led us to choose four operating modes: a `manual` mode for teaching; an `automatic` mode for harvesting; a `reconfiguration` mode for crossing the elbow singularity; and a `free` mode for safety requirements. In the `manual` mode, the arm is compliant (the desired effort is set to zero) and can be programmed using a teaching-by-showing procedure. The surgeon moves the robot on the initial pose on skin, then on the final pose by holding the dermatome handle and activating the DMS. The poses are successively recorded (or deleted) by pressing on the $+$ (or $-$) button. The teaching sequence is validated (or deleted) by pressing the `enter` (or `esc.`) button, which switches the system in the `automatic` mode: first, the surgeon selects a desired force for harvesting (from 0 up to 100 N); then, as soon as he activates the DMS, the dermatome motor is switched on and the robot starts the harvesting sequence as indicated in Fig. 6. The `free` mode enables the surgeon to move the robot without force control thanks to the backdrivability of the shoulder. Any motion within the joint limits can be performed since no axes are controlled. This mode can be used to push the arm away from the patient in case of emergency or to drive it in a parking position.

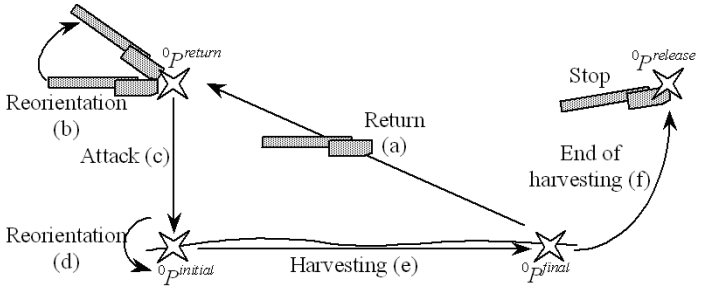

Fig. 6. Different steps of motion during the `automatic` mode.

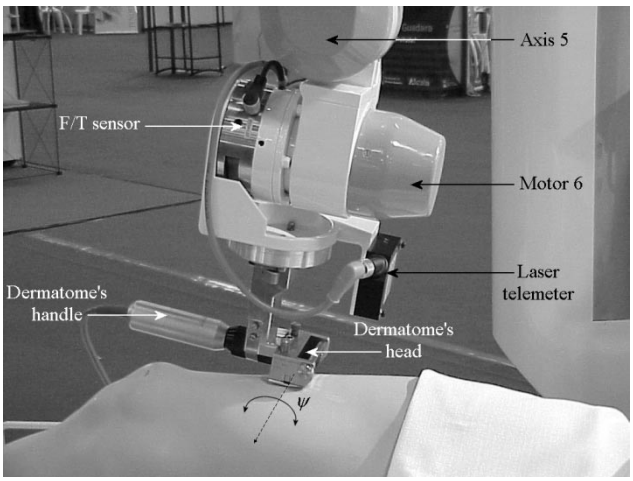

Fig. 7. Close-up of the Dermarob wrist.

B. Force/Torque Measurement

The application requires force control to move the arm in both manual and automatic modes. The wrist (Fig. 7) is equipped with a six-component F/T sensor (Gamma transducer from ATI which allows measuring up to 130 N and 10 Nm with a resolution of 0.012 N and 0.0003 Nm). Experiments on a nonplanar surface covered with foam rubber and coated with silicon have shown that the F/T sensor was unable to measure the torque M_y about y accurately enough. Thus, it is not possible to control the pitch angle ψ, even on a flat surface, since a bump (function of the contact force F_z) is developing ahead of the dermatome. Therefore, a laser telemeter has been added to measure the distance d between the wrist and the skin (Fig. 7). Before starting the harvesting process (step 3), a reference measurement, d_{ref}, is acquired. M_y is then estimated by the following simple observer, where k is a gain factor

$$M_y = k(d - d_{\text{ref}}). \tag{1}$$

The trajectories of ψ and M_y when harvesting on a spherical surface are shown in Fig. 8. A steady-state region can be observed at 10 s on the pitch angle with the laser telemeter because after the reorientation step (step d, Fig. 6), the robot has to wait a few seconds for the efforts to be stabilized before beginning the harvesting motion.

C. Force Control

Force control has been widely addressed in the past, and state of the art can be found, for instance, in [15]. The most commonly

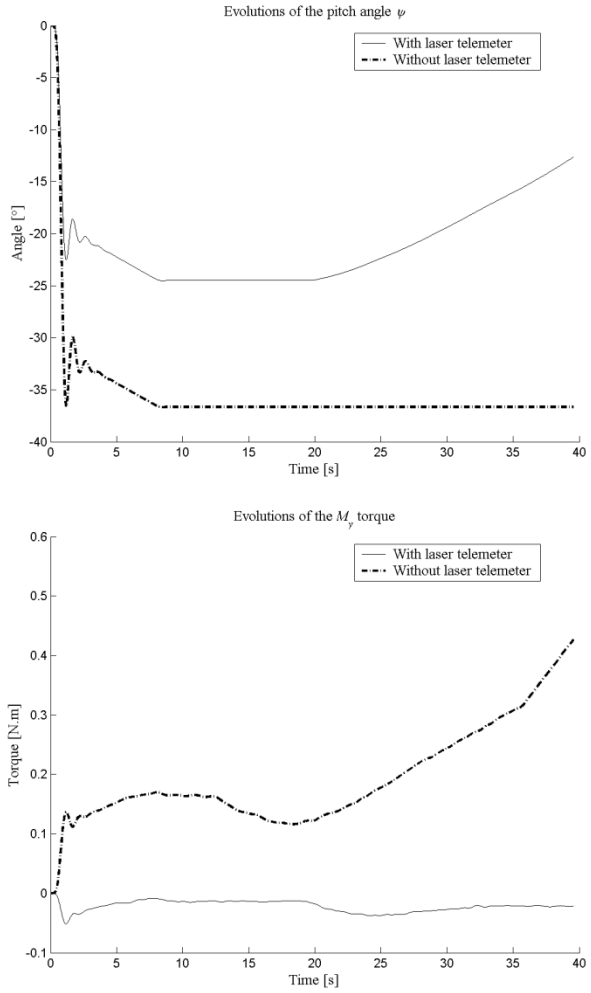

Fig. 8. Comparison of harvesting on a spherical surface with and without controlling the pitch angle.

used methods are [14] those involving the relation between position and applied force (passive stiffness control [16] and active stiffness control [17]), those using the relation between velocity and applied force (impedance control [18]), and those using position and force feedback (parallel hybrid control [19] and external hybrid control [20]).

As previously mentioned, due to the task constraints, a force control with force measurement is needed. Thus, the first kind of method is discarded since it does not make use of F/T measurements. Among the remaining controls, impedance and parallel hybrid have also been discarded. Indeed, with the first one, it is not possible to prescribe a desired wrench. Then, the second one enables either force control or position control along a given direction, but not both. The external hybrid control, composed of two embedded control loops, is the only suitable one for the application at hand. Here again, different schemes have been proposed depending on the space where the summation of components is achieved (addition of joint torques, velocities, or forces) and on the position control (joint control by IGM or Jacobian matrix, and Cartesian control).

External control with Cartesian summation between force and position components as well as joint control by IGM have been chosen. The block diagram of Fig. 9 illustrates how the controller

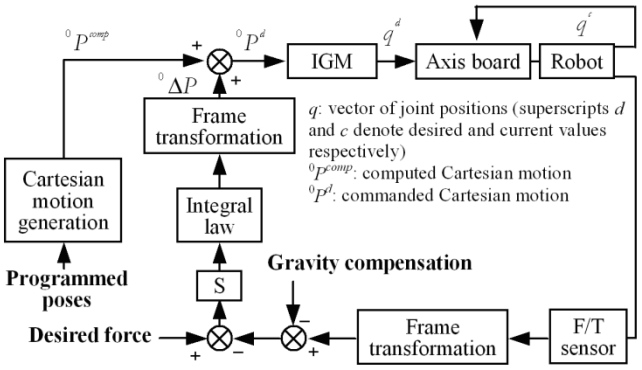

Fig. 9. External hybrid force-position control scheme.

works [21]. After appropriate transformation, the difference between the desired and measured forces gives an increment $^0\Delta P$ which is used to modify the desired motion $^0P^{\text{comp}}$ computed by the motion generator. S is a selection matrix that allows the surgeon to select the Cartesian directions along or about which the force and moment will be controlled. The closed-form solution of the IGM computes the joint positions sent to the axis board (a PMAC-PC board from Delta Tau).

The key advantages of such a scheme can be summarized as follows [22]: 1) the joint position servo loop is always activated, providing stability and avoiding switching between the position loop and the force loop; 2) its performance is very satisfying with simple and reliable (thus safe) control laws (such as a proportional-integral-derivative (PID) at the joint level and an integral law for the external force loop); 3) it is easy to implement on any kind of controller; 4) unless an effort is applied on the dermatome (below the force sensor), the robot will not move; and 5) the control software can be incrementally designed, facilitating the tuning of the parameters and validation (internal joint control, then external Cartesian space control, and finally additional force-control loop). This cascade structure provides a more robust control.

D. Controller Safety

The hardware and software safety features are presented below.

1) Hardware Safety: A watchdog board has been developed in order to manage safety from a software point of view. If anything goes wrong in the high-level controller, the cyclic signal sent to the watchdog is stopped, inactivating it and switching off the power. In order to improve safety, two redundant circuits have been wired on the board. Each external module—F/T sensor, laser telemeter, and motors—is controlled by a specific board. Each one is separately initialized and can detect a fault on the module: for the first board, disconnection, saturation, or incoherent data of the F/T sensor; for the second board, laser measurement out of range; and for the third board, tracking error during the arm motion, excessive velocity on a motor, translator or amplifier failure, arm close to the limit of workspace. Moreover, several LEDs on the console desk and on the arm are there to warn users of any fault while in motion.

2) Software Safety: The high-level program has been built using a safety-based software analysis. Five QNX processes are

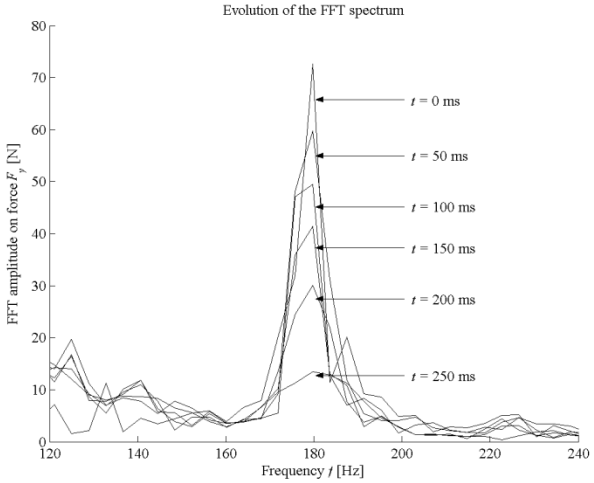

Fig. 10. Spectral density of the dermatome motor as a function of time after a blade jamming at $t = 0$ $(M = 256)$.

running, one for each specific task: security; operating modes; force; communication; and translator controls. They run accordingly to a round-robin mode and communicate using shared-memory variables in the data bases. Each one can be read or written by authorized processes only. Of course, the safety variables have a higher priority than the other ones. If no fault occurs, the five processes are running within a sampling period of 1 ms. Moreover, every time a fault occurs, all software and hardware systems are reinitialized. Besides, in addition to the aforementioned hardware watchdog, the dedicated security process checks the activity of the other ones. If one is locked, then the emergency procedure is switched on.

In a fault occurs, or if the DMS pedal is switched off during the `automatic` mode, different phases of clearing have been planned depending on whether the blade is in contact with the skin or not.

Finally, in order to detect a blade jamming that can occur during the skin harvesting (due, for example, to a bad lubrication of the mechanism) which would cause a tearing of the skin, a fast Fourier transform (FFT)-based algorithm has been implemented. It relies on the analysis of the dermatome noise, namely, on the tracking of the resonance frequency f_d of the blade. Indeed, as soon as the motor is switched on, vibrations caused by the blade oscillations can be observed on the F_y component of the F/T sensor. Computed on the M last data samples, an FFT allows to observe the blade oscillations, as shown in Fig. 10, for a motor speed of about 11 000 rpm $(f_d = 180$ Hz). Experimental studies have shown that with appropriate data analysis, it was possible to obtain a robust detection of blade jamming with respect to measurement noise together with an acceptable response time (typically 100 ms). Thus, with a robot's maximum velocity of 10 mm/s, the dermatome would move for less than 1 mm, which is quite reasonable considering the skin elasticity.

VI. Experimental Results

To validate the mechanical structure and the high-level control, Dermarob has been tested by a surgeon in clinical conditions on anaesthetized pigs (Fig. 11). The operations have been

(a)

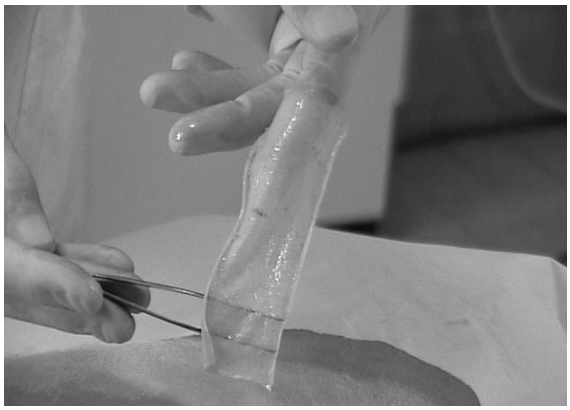

(b)

Fig. 11. (a) Experimental test on a pig and (b) the resulting skin graft.

performed at the Experimental Surgery Laboratory, School of Medicine, Montpellier, France. For these tests, the desired force was set up to 35 N, which is smaller than the values found during the feasibility study. As a matter of fact, in the manual procedure, the surgeon exerts a force higher than necessary to make sure that the skin sample will have a regular shape and no hole.

In these tests, Dermarob harvested samples estimated by the surgeon to be of same quality as those he would have obtained manually. This "visual" macroscopic appreciation of the quality will be quantified more precisely in future experiments. Samples will be sent to an anatomopathology lab to measure the regularity of thickness over a whole graft. The quality of the graft at a microscopic level will also be checked. However, we expect no change since the dermatome held by Dermarob is the same device as the one manually used by the surgeon.

Fig. 12 shows the trajectory of the Cartesian position of the dermatome along z with respect to time as well as pitch and roll angles about y and x, respectively. Fig. 13 shows the corresponding trajectories of forces and moments.

The different zones in these figures should be interpreted as follows (see also Fig. 6): a) the robot approaches the first programmed location (no contact): no force control is required and only the Cartesian generation is activated; b) after a 10° reorientation about y (experimental value), the force control is switched on along z and the Cartesian generation is switched off; c) the dermatome moves down until the skin contact force F_z^c reaches the desired force F_z^d and the dermatome motor is started up; d)

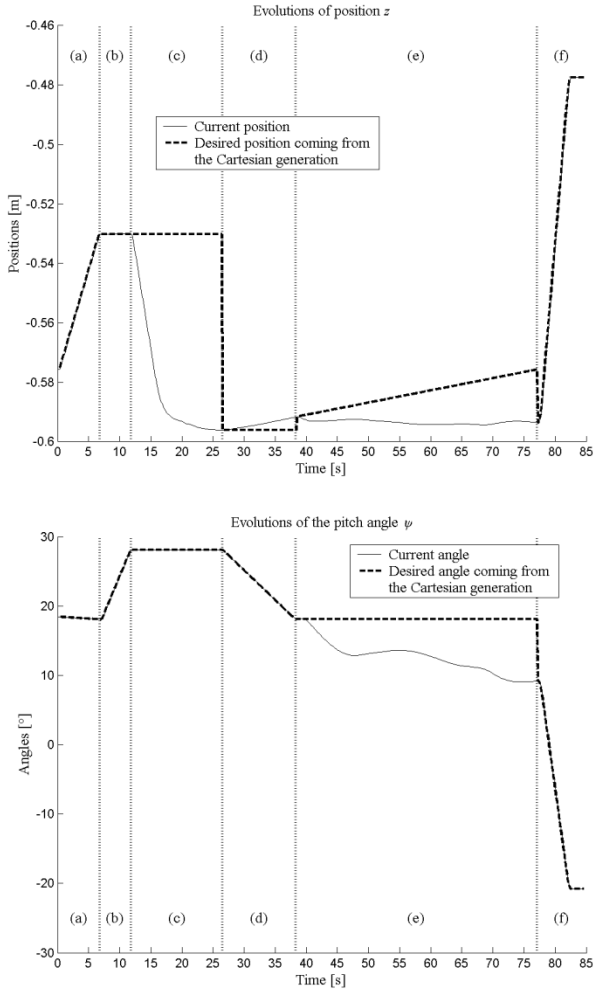

Fig. 12. Position (above) and angle (below) trajectories during a motion.

thanks to a reorientation about y of -10°, the blade begins to cut the skin; e) the harvesting motion starts under force control along z to control the force applied on the skin, and about x to control the roll angle; the pitch angle about y is controlled using the laser telemeter; the Cartesian motion along x is a simple interpolation between the two preplanned locations; and f) when the dermatome reaches the final programmed location, the force control is switched off, the velocity of the Cartesian motion increases, and the blade is freed from the skin by a quick pitch motion which tears the skin strip.

VII. Discussion

1) The mechanical, hardware and software safety features embedded in Dermarob make the system intrinsically safe. A risk analysis shows that, when a low-level fault is detected by the software, it takes 2.5 ms in the worst case to switch off the power. In case of a high-level fault handled through the watchdog board, the robot is stopped within 10 ms. At maximum velocity (10 mm/s), it represents a maximum displacement of 0.025 mm in the first case, and of 0.1 mm in the second one. Such a motion is too small to produce a force large enough to cause any harm to the patient or the operator.

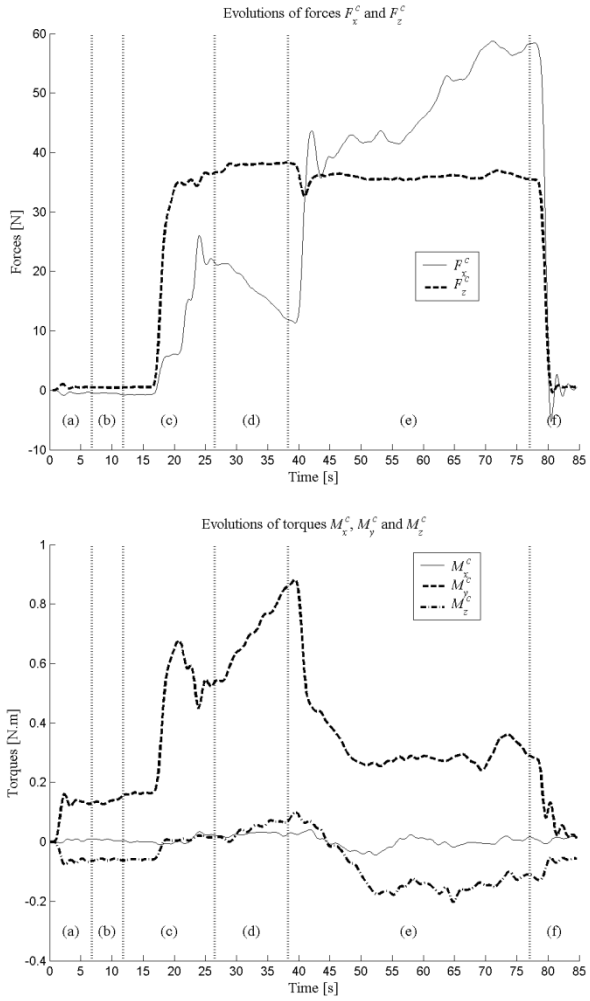

Fig. 13. Force (above) and torque (below) trajectories during a motion.

2) Experiments have shown that an additional force control along the direction of motion x is mandatory to better cope with the bump ahead of the dermatome and to better control the motion when the compliance of the skin is not constant along a given path (due to the presence of ribs, for instance, when harvesting on the back). This can be easily achieved with the selection matrix of the chosen control structure.
3) The geometric parameters of the models have been approximated from the robot data sheets. In order to improve performance, an appropriate calibration procedure will be performed.
4) A path generator based on a higher order polynomial is under development in order to take via points into account. The goal is to harvest skin grafts of complex shapes.
5) Currently, the team is working on biomechanical models of skin which are intended to improve the harvesting process. Unlike usual visco-elastic models, which consider only the contact direction z, this analysis is extended to the motion direction along x [24]. With such a model, a procedure could be run in the OR before starting to harvest in order to identify the model parameters and to better tune the control law parameters according to the skin characteristics of the patient.

VIII. Conclusion

This paper presented Dermarob, the first robotic system dedicated to skin harvesting in reconstructive surgery. Considering surgeon's gesture and safety constraints, a SCARA active robot with a nonspherical wrist has been designed. The robot is position-force controlled and is easily handled, thanks to a user-friendly interface. Special care has been attached to safety at mechanical, hardware, and software levels. The project is currently under validation: experiments have been run on pigs, showing that the performance of the robot was qualitatively equivalent to the performance of the surgeon. Additional experiments will be run to clinically confirm this evaluation. Once the improvements suggested in the discussion have been implemented, further work will consider experiments on cadavers before trying for *in vivo* harvesting at a later stage.

References

[1] J. P. Trevelyan, *Robots for Shearing Sheep: Shear Magic*. Oxford, U.K.: Oxford Univ. Press, 1992.
[2] F. Pierrot, E. Dombre, E. Dégoulange, L. Urbain, P. Caron, S. Boudet, J. Gariépy, and J.-L. Mégnien, "Hippocrate: A safe robot arm for medical applications with force feedback," *Med. Image Anal.*, vol. 3, no. 3, pp. 285–300, 1999.
[3] S. E. Salcudean, G. Bell, S. Bachmann, W. H. Zhu, P. Abolmaesumi, and P. D. Laurence, "Robot-assisted diagnostic ultrasound—Design and feasibility experiments," in *Proc. 2nd Int. Conf. Medical Image Computing and Computer-Assisted Intervention (MICCAI)*, Cambridge, U.K., 1999, pp. 1062–1071.
[4] F. Pierrot, E. Dombre, L. Téot, and E. Dégoulange, "Robotized reconstructive surgery: Ongoing study and first results," in *Proc. IEEE Int. Conf. Robotics and Automation*, San Francisco, CA, 2000, pp. 1615–1620.
[5] B. L. Davies, "Safety of medical robots," in *Proc. Int. Conf. Advanced Robotics (ICAR)*, Tokyo, Japan, 1993, pp. 311–317.
[6] M. Fadda, T. Wang, B. Allota, P. Dario, M. Marcacci, and S. Martelli, "Safety requirements in a robotic surgical system: First analysis and approach," in *Proc. 3rd Int. Symp. Measurement and Control in Robotics*, Torino, Italy, 1993, pp. 21–24.
[7] S. Lavallée, J. Troccaz, L. Gaborit, P. Cinquin, A. L. Benabid, and D. Hoffman, "Image-guided robot: a clinical application in stereotactic neurosurgery," in *Proc. IEEE Int. Conf. Robotics and Automation*, Nice, France, 1992, pp. 618–625.
[8] H. A. Paul *et al.*, "Development of a surgical robot for cementless total hip arthroplasty," *Clinical Orthopaedics Related Res.*, vol. 285, pp. 57–66, 1992.
[9] J. Troccaz and Y. Delnondedieu, "Semi-active guiding systems in surgery. A two-DOF prototype of the passive arm with dynamic constraints," *Mechatronics*, vol. 6, pp. 399–421, 1996.
[10] S. J. Harris *et al.*, "Experiences with robotics systems for knee surgery," in *Proc. CVRMed-MRCAS'97*, Grenoble, France, 1997, pp. 757–766.
[11] E. Dombre, P. Poignet, F. Pierrot, G. Duchemin, and L. Urbain, "Intrisically safe active robotic systems for medical applications," in *Proc. 1st IARP/IEEE-RAS Joint Workshop Technical Challenge for Dependable Robots in Human Environments*, Seoul, Korea, 2001, Paper III-4.
[12] G. Duchemin, E. Dombre, F. Pierrot, and E. Dégoulange, "SCALPP: A 6-DOF robot with a nonspherical wrist for surgical applications," in *Advances in Robot Kinematics*, J. Lenarcic and M. M. Stanisic, Eds. Dordrecht, The Netherlands: Kluwer, 2000, pp. 165–174.
[13] D. L. Pieper, "The kinematics of manipulators under computer control," Ph.D. dissertation, Stanford Univ., Stanford, CA, 1968.
[14] W. Khalil and E. Dombre, *Modeling, Identification and Control of Robots*. London, U.K.: Hermes Penton, 2002.
[15] T. Yoshikawa, "Force control of robot manipulators," in *Proc. IEEE Int. Conf. Robotics and Automation*, San Francisco, CA, 2000, pp. 220–226.

[16] J. L. Nevins *et al.*, "Exploratory Research in Industrial Modular Assembly," Charles Stark Draper Lab., Cambridge, MA, Rep. R-1111, 1977.
[17] K. Salisbury, "Active stiffness control of a manipulator in Cartesian coordinates," in *Proc. 19th IEEE Conf. Decision and Control*, Albuquerque, NM, 1980, pp. 95–100.
[18] N. Hogan, "Impedance control: An approach to manipulation," *J. Dynam. Syst., Meas., Contr.*, vol. 107, pp. 1–24, 1985.
[19] M. H. Raibert and J. J. Craig, "Hybrid position/force control of manipulators," *J. Dynam. Syst., Meas., Contr.*, vol. 103, pp. 126–133, 1981.
[20] J. De Schutter and H. Van Brussel, "Compliant robot motion—II: A control approach based on external control loop," *Int. J. Robot. Res.*, vol. 7, no. 4, pp. 18–33, 1988.
[21] G. Duchemin, E. Dombre, F. Pierrot, and P. Poignet, "Skin harvesting robotization with force control," in *Proc. Int. Conf. Advanced Robotics (ICAR)*, Budapest, Hungary, 2001, pp. 101–106.
[22] V. Perdereau and M. Drouin, "A new scheme for hybrid force-position control," *Robotica*, vol. 11, pp. 453–464, 1993.
[23] E. Dégoulange, P. Dauchez, and F. Pierrot, "Determination of a force control law for an industrial robot in contact with a rigid environment," in *Proc. IEEE Conf. Systems, Man and Cybernetics*, vol. 2, Le Touquet, France, 1993, pp. 270–275.
[24] G. Duchemin, E. Dombre, F. Pierrot, and P. Poignet, "Robotized skin harvesting," in *Experimental Robotics VIII, Springer Tracts in Advanced Robotics*, B. Siciliano and P. Dario, Eds. Berlin, Germany: Springer-Verlag, 2003, vol. 5, pp. 404–413.

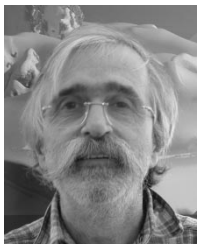

Etienne Dombre (M'02) received the Ph.D. degree in automatic control in 1975 and the "Thèse d'Etat" in 1981, both from University of Montpellier, France.

He is a Director of Research with CNRS (French National Scientific Research Center), currently in the Laboratoire d'Informatique, Robotique et Microélectronique de Montpellier (LIRMM), Montpellier, France, where he is Head of the Robotics Department. His current research interest is in medical robotics.

Gilles Duchemin received the M.S. degree in microelectronics and automatics engineering, from the Engineering Sciences Institute of Montpellier, France in 1999 and the Ph.D. degree in automatic control from the University of Montpellier, Montpellier, France in 2002.

He is currently a Postdoctoral Fellow at the Laboratoire d'Informatique, Robotique et Microélectronique de Montpellier (LIRMM), Montpellier, France.

Philippe Poignet received the M.E. and Ph.D. degrees in control engineering from the University of Nantes, Nantes, France in 1992 and 1995, respectively.

From 1996 to 1998, he was with SEPRO Robotics Company, France. From 1998 to 2000, he was Assistant Professor at the University of Orleans, Orleans, France. He joined the Laboratoire d'Informatique, Robotique et Microélectronique de Montpellier (LIRMM), Montpellier, France, in 2000 and is currently Assistant Professor at the University of Montpellier II, Montpellier, France. His research interests include robot identification, nonlinear control, and the applications to medical robotics and artificial locomotion.

François Pierrot (M'93–SM'98) received the M.S. degree in mechanical engineering from the University of Paris, Paris, France, in 1986 and the Ph.D. degree in automatic control from the University of Montpellier, Montpellier, France, in 1991.

He has been with Laboratoire d'Informatique, Robotique et Microélectronique de Montpellier (LIRMM), Montpellier, France, since 1991, as a Researcher, Senior Researcher (1996), and Director of Research (2002) from CNRS (French National Scientific Research Center).